



Experimental Investigation of Concrete-Filled Double Steel Tube Columns (CFDST) with High Performance Materials Under Monotonic and Cyclic Loading

Dennis Witteck¹✉, Rebekka Winkler², and Markus Knobloch²

¹ Institute for Structural Engineering, Structural Testing Laboratory,
Ruhr-Universität Bochum, Bochum, Germany
dennis.witteck@rub.de

² Institute of Steel, Lightweight and Composite Structures, Ruhr-Universität
Bochum, Bochum, Germany
{rebekka.winkler, markus.knobloch}@rub.de

Abstract. This paper presents an experimental study on the performance of innovative Concrete-filled double steel tube (CFDST) columns with high-performance building materials under monotonic and cyclic loading. In total six stub CFDST-columns and two conventional stub concrete-filled steel tubes (CFST) were tested at Ruhr-Universität Bochum under a constant axial load with either a monotonic or a cyclic increase of lateral displacement.

Focus of the paper is the comparison of the characteristic behavior of the specimen like the hysteric behavior, ductility and energy dissipation. The experimental investigations have shown that the resistances, ductility and energy dissipation of innovative CFDST is increased compared to conventional CFST-columns. The use of a high-strength inner tube did show the most benefits in terms of the resistances, while at the same time a configuration with normal-strength core materials showed better results in terms of the energy dissipation and ductility.

Keywords: Experimental study · Concrete filled steel tubes · Seismic design · Ductility

1 Introduction

Concrete filled composite (CFST) columns made of normal-strength materials have proven their suitability under seismic loading in engineering practice over the last decades, and their high resistance has been confirmed in several research projects e.g. [1–4]. A further development of these type of composite columns are concrete filled double steel tubes (CFDST) - columns with high strength building materials. These types of columns consist of an outer and an inner steel tube. The gap between the outer and inner tube as well as the inner tube itself are both filled with concrete. In comparison to conventional composite columns the external dimensions can be reduced while maintaining the same load-bearing capacity and due to the prefabrication in factories the time required to erect individual floors is minimized while the manufacturing tolerances meet the standards for steel structures.

The load bearing behaviour of these innovative columns with high performance materials has already been investigated at ambient temperatures and in case of fire [5–7]. On the other hand, CFDST-columns with high performance materials are not yet implemented in standards [8, 9] and, in particular, the seismic performance has not been comprehensively investigated so far.

In this paper, the experimental results of three test series of CFDST-columns and one test series of CFST-columns under cyclic loading are presented. The columns were tested under bi-axial loading at the Ruhr-Universität Bochum. The cyclic performance of the composite columns is evaluated in terms of hysteric behaviour, ductility and energy dissipation.

2 Experimental Program

2.1 Test Specimen

In this study a total of eight specimens were tested with a total length of 1,500 mm, Table 1. Six specimens were manufactured as CFDST-columns (no. 1 to 6) with normal and high-performance materials, two specimens were manufactured as CFST-columns (no. 7 and 8) with normal strength materials. These columns were used as reference to evaluate the performance of the CFDST-columns. The outer tube had a diameter of 273.0 mm and a wall thickness of 8.8 mm. Only normal strength steel was used. The inner tube had the same wall thickness and a diameter of 177.8 mm. Both grade S355 and S770 steels were used.

Table 1. Properties of the tested specimens

Specimen no.	Ø 273.0 × 8.8 mm f_y [N/mm ²]	Ø 177.8 × 8.8 mm f_y [N/mm ²]	$f_{ck,cube}$ [N/mm ²]	Total length [mm]
1&2	385	815	53.6	1,500
3&4	385	815	115.6	1,500
5&6	385	385	54.8	1,500
7&8	385	–	52.1	1,500

The columns were manufactured from steel tubes of the same batch. For each batch three tensile specimens were tested. The compression strengths of the concrete specimens were tested at the same day as the tests of the columns using three cube specimen per batch. Table 1 shows the mean values of the material characterization test results and the dimensions of each column.

2.2 Test Setup and Measurement Equipment

The test setup was arranged in a 20 MN universal testing machine (Fig. 1). A lateral actuator (1,000 kN/±125 mm capacity) was fixed in horizontal orientation with hinges at both ends (cardan joints) and centered to the intermediate plate. A sliding plate (stainless steel) and a greased UHPWE-layer was added beneath the tested specimens.

Between the foot of the columns and the intermediate plate, a bolt joint was installed to enable rotation during the horizontal movement. The head of the specimens is centered in a stiffened steel quiver ($2 \times \text{HEB400}$), filled with grout mortar and connected to the crosshead of the machine. The length of the quiver clamping was $l = 500 \text{ mm}$. The free length of the specimen was $1,000 \text{ mm}$.

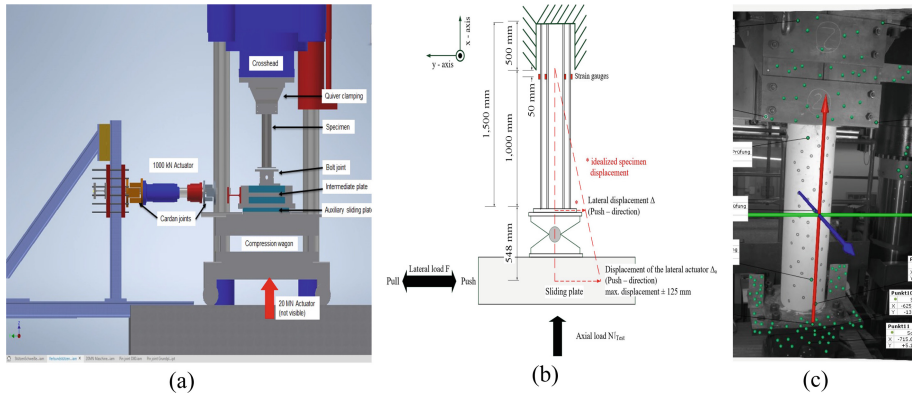


Fig. 1. (a) Test setup, (b) schematic setup, (c) view of the DIC – system

The displacement and rotation of the test specimens and the setup components were measured by means of digital image correlation (DIC) (Fig. 1c). On each tube two strain gauges were installed 50 mm outside of the quiver clamping.

2.3 Loading Protocol

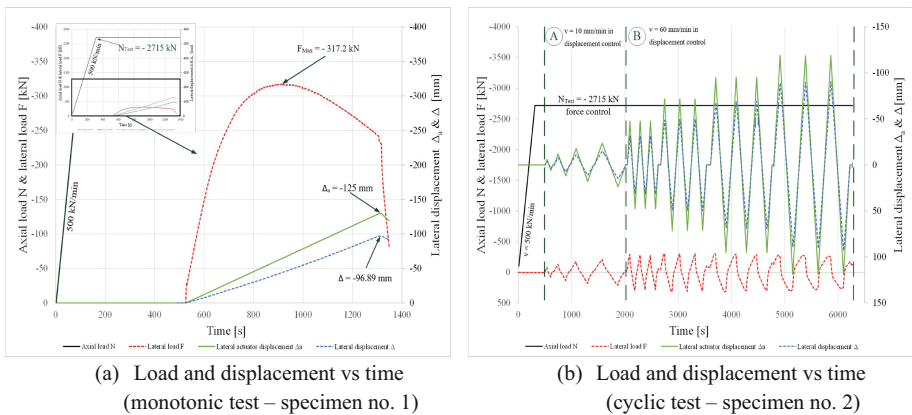


Fig. 2. Monotonic and cyclic test curves of specimen no. 1 and 2

The tests were performed according to the loading protocol presented in [10]. An overview of the loading parameters is given in Table 2. Figure 2 illustrates with the axial load time-histories of specimens no. 1 (monotonic) and 2 (cyclic) the loading

protocol. The specimens were first continuously loaded by an axial load (i.) up to $N_{\text{Test}} = 0.3 N_{\text{pl}}$, which is the axial load limit in columns design according to [8].

Table 2. Loading parameters

Specimen no.	1	2	3	4	5	6	7	8
Loading type	(a)	(b)	(a)	(b)	(a)	(b)	(a)	(b)
Axial load ratio $N_{\text{Test}}/N_{\text{pl}}$	0.3							
Axial load N_{Test} [kN]	-2715		-3568		-2081		-1568	

(a) Monotonic loading, (b) Cyclic loading

The plastic resistance N_{pl} was calculated according to Eurocode 4 [9] with the mean values of the material tests listed in Table 1. From this point on forward, the axial load N was kept constant in load control and the lateral displacement Δ_a (ii.) was applied displacement-controlled. For each parameter set of the cross-section dimensions two loading types for the lateral displacement Δ_a were considered – (a) a monotonic test (Fig. 2a) and (b) a cyclic test (Fig. 2b). In the monotonic load test (a), the specimens were continuously loaded up to the maximum lateral actuator displacement Δ_a of ± 125 mm. The monotonic-test was used to determine the displacement Δ_y corresponding to the yield load F_y as input value for the definition of the cyclic loading protocol. In the cyclic loading part (b) the loading was performed with incremental increase of the displacement Δ_y until the maximum actuator displacement of $\Delta_a = \pm 125$ mm was reached (see Fig. 2b).

3 Results

3.1 Accuracy of the Test Facility

The quality of the specimens mounting in the test apparatus was examined. Figure 2 shows, as an example, additional to the control (primary) parameters of the tests (continuous lines) the evolution of the measured (secondary) parameters, like the lateral load F (red) and the lateral specimen displacement Δ (blue) (dotted lines) over the course of the test time. The lateral load axis was 548 mm under the foot of the specimens (Fig. 1d). Therefore, the actual specimen displacement Δ result smaller than the actuator displacement Δ_a (eg. Fig. 2a, $\Delta_{\text{Specimen,no.1,max}} = -96.89$ mm). The comparison between the primary and secondary parameter curves illustrates an immediate load application without any slippage in the setup.

3.2 Hysteretic Behaviour

The hysteretic behaviour of the columns is analysed in terms of lateral load F vs. displacement Δ curves, where the events yielding, reaching the ultimate load F_{max} and reaching 80% of F_{max} are separately marked (Fig. 3). The corresponding values are presented in Table 3. The characteristic phases of the hysteric loops are plotted in red (elastic), blue (non-linear behaviour) and green (post ultimate range).

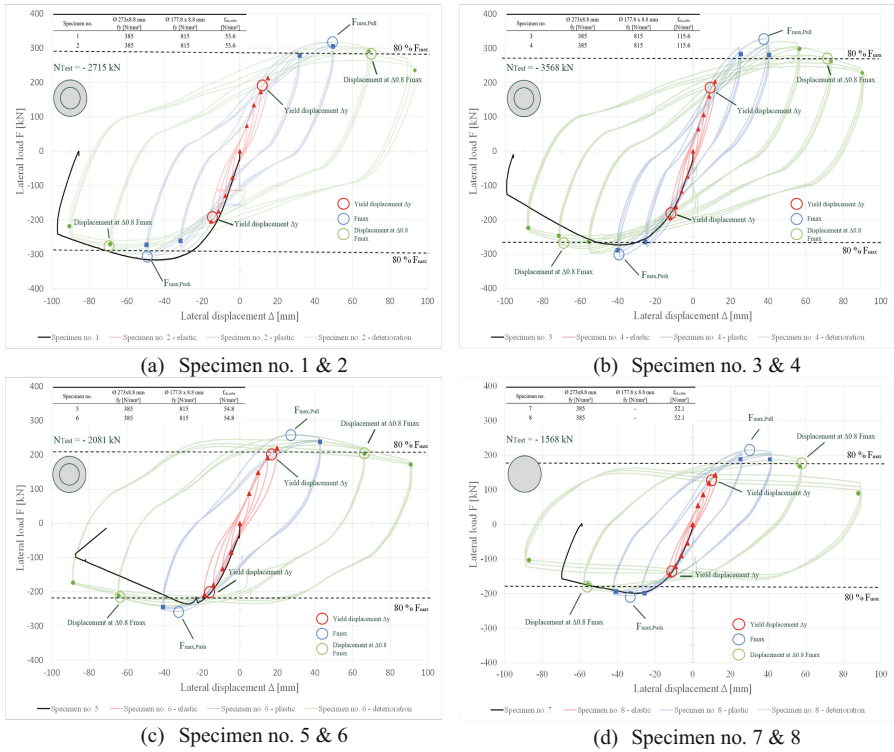


Fig. 3. Lateral load F vs. displacement Δ

Generally, the CFDST showed good resemblance to the CFST in the shape of hysteresis curves (Fig. 3a to c vs. 3d), implying that the CFDST-column type had a global cyclic response akin to that of the CFST-type. All specimens showed a symmetrical and ductile behaviour during the cyclic loading. In addition, the CFDST-columns (no. 2, 4, 6) exhibited a fuller hysteretic curve compared to the CFST (no. 8), indicating a better energy dissipation capacity (Fig. 4).

Table 3. Lateral displacements and ultimate lateral load

Specimen no.	Monotonic tests			Cyclic tests					
	Δ_y [mm]	F_{max} [kN]	$\Delta_{80\% F_{max}}$ [mm]	Δ_y [mm]		F_{max} [kN]		$\Delta_{80\% F_{max}}$ [mm]	
				Push	Pull	Push	Pull	Push	Pull
1&2 (CFDST)	-15.61	-317.2	-88.81	-15.29	+14.97	-305.2	+317.2	-84.36	+85.69
3&4 (CFDST)	-15.07	-273.8	-77.42	-14.46	+14.24	-305.6	+328.7	-67.78	+73.55
5&6 (CFDST)	-18.96	-234.2	-50.85	-13.95	+14.80	-257.7	+260.5	-63.88	+65.57
7&8 (CFST)	-13.38	-199.1	-77.36	-12.21	+11.86	-206.5	+214.9	-55.77	+56.30

Each column displayed material softening under repeated loading at the same displacement. The use of a high-strength inner tube increases the stiffness and lateral load capacity F_{max} (no. 2 and 4) compared to specimen no. 6 (S355 inner tube) or specimen no. 8 (CFST). While at the same time the influence of the high-strength concrete had less influence on the lateral load capacity by comparing specimen no. 2 and 4 (see Table 3).

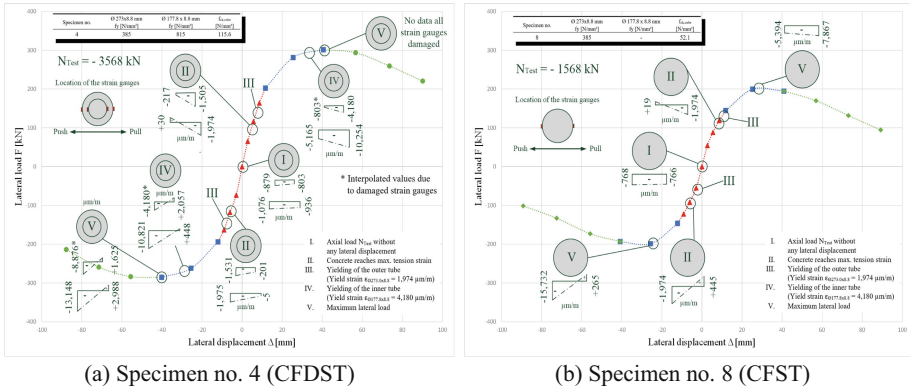


Fig. 4. Envelope curves and strain distributions for specific events

The differences in cyclic behaviour of the CFDST and the CFST is analysed in terms of lateral load F versus lateral displacement Δ envelope curves of specimen no. 4 and 8 (Fig. 4). The lateral stiffness and ultimate lateral load F_{max} were positively affected by the inner steel tube. The comparison of the envelope curves displays an increase in stiffness and of the ultimate load F_{max} . The post ultimate behaviours of both types can be regarded as highly ductile, while no. 4 exceeds the ductility of no. 8 despite the high strength core materials. The envelope curves (Fig. 4) describe a mostly symmetrical behaviour under cyclic loading with slight deviations resulting from geometric imperfections and after the initial buckling of the specimens.

The measured strain distribution of key events (I–V) during the cyclic tests are displayed in Fig. 4. Event (I) marks the point when the axial load N_{Test} was applied ($F = 0$). The effect of the geometric imperfections on the strain distribution is shown by inclination the in the distribution on each tube. For the CFDST a difference in stain was measured between the inner and outer tube indicating a gap between the inner tube and base plate of the clamping. In event (II) the outer steel tube reached its yield limit of $\epsilon_{yield, S355} = \pm 1,974 \mu\text{m/m}$. Because of the higher axial load N_{Test} , of specimen no. 4, the yield limit was reached already at a displacement of $\Delta_{II, no.4} = -6.77/+7.09 \text{ mm}$ compared to corresponding displacement of specimen no. 8 $\Delta_{II, no.8} = -8.41/+7.33 \text{ mm}$. After the yielding of the outer tube the load shifts to the inner steel tube (no. 4), which is still elastic at this point of the loading (II). At event (III) the maximum concrete tension strain of $100 \mu\text{m/m}$ was reached. This point was calculated indirectly by strain gauge measurements on the tubes. As shown at (I) the axial loads lead to

different compression strain levels between the two specimens. Due to the bending moment applied resulting from the lateral displacement, the CFST-column reached event (III) before its tube began to yield (II). For the no. 4 the behaviour was reversed. With further loading the F over Δ curve of the CFDST-specimen begins to slowly show a non-linear behaviour until the inner tube starts to yield (IV) at a strain of $\epsilon_{yield, S770} = -4,180 \mu\text{m/m}$. Shortly after event (IV) the maximum lateral load F_{max} (V) is reached. The CFST (no. 8) had no additional inner tube and could no redistribute the load, a bent in the envelope curve can be observed between point (II) and (III) until the maximum load $F_{max,no.8}$ is reached (V).

3.3 Comparison and Evaluation

The specimen’s ductility μ is defined as the ratio between yield displacement Δ_y and the lateral displacement $\Delta_{80\% F_{max}}$ at 80% of the ultimate lateral load F_{max} . Figure 5a presents the cyclic ductility μ for the cyclic tested columns for both load directions. The values of all columns resulted between 4.43 and 5.72. The overall ductility μ of the CDFST-columns is comparable or exceeds the ductility μ of the CFST-specimen and can be regarded as highly satisfactory. According to [4] the ductility of columns can be rated as “very good”, if the value μ is >5.0 .

The dissipated energy per cycle (EDC) is defined as the area of the F vs. Δ – curve shown in Fig. 3. Figure 5b shows the actual EDC (dotted lines) as well as the normalized EDC related to the CFST-column (no. 8) (continuous lines). The lowest amount of energy is dissipated by the CFST-column (no. 8). The largest amount of energy was dissipated by CFDST-column (no. 6), with up to 3.2 times the energy of no. 8 at a displacement ratio of 2.0. The EDC values of specimens no. 2 and no. 4 were between the extremes of the normal strength CFST and CFDST-column. The reason for that was the higher yield limit of the S770 inner tube. The results show that normal strength core materials are more beneficial for energy dissipation compared to the high-strength core materials. Nevertheless, all CFDST-specimens independent from there material configuration exceeds the dissipation capacity of tested normal strength CFST-specimen.

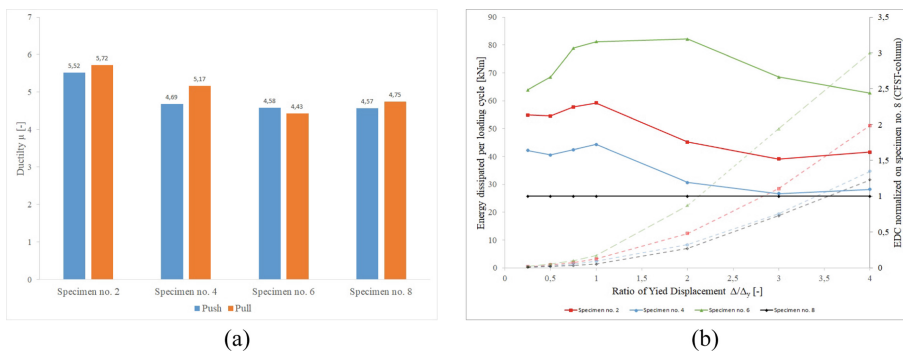


Fig. 5. (a) Ductility μ and (b) EDC of the columns

4 Conclusion

In this experimental study six CFSDT-columns with normal and high-strength materials and two CFST-columns with normal strength materials were tested. The following conclusions can be drawn regarding the performance of the normal and high strength CFDST-columns compared to normal strength CFST-columns: I) The axial and lateral load bearing capacity of normal and high strength CFDST-columns is higher than the capacity of the tested normal strength CFST-column. II) The ductility μ of the tested CFDST-columns is on the same level or surpasses the CFST-column despite the use of the high-performance materials. III) The additional steel tube of the CFDST-columns leads to an increased energy dissipation capacity compared to the CFST-column.

References

1. Huang Y (2015) Seismic behavior of concrete filled steel tubular built-up columns. University of Trento
2. Varma A, Ricles J, Sause R, Lu L (2002) Seismic behaviour and modelling of high-strength composite concrete-filled steel tube (CFT) beam-column. *J Constr Steel Res* 58:725–758
3. Qin P, Xiao Y (2013) Research on concrete-filled steel tube columns subjected to cyclic lateral force. In: The 2012 world congress on advances in structural engineering and mechanics (ASEM 2013) Jeju, Korea, 8–12 September 2013
4. Susantha KAS, Aoki T, Hattori M (2008) Seismic performance improvement of circular steel columns using precompressed concrete-filled steel tube. *J Constr Steel Res* 64:30–36
5. Portolés JM, Romero ML, Bonet JL, Filippou FC (2011) Experimental study of high strength concrete-filled circular tubular columns under eccentric loading. *J Constr Steel Res* 67:623–633
6. Romero ML et al (2016) Circular concrete-filled dual steel columns with ultrahigh-strength concrete. *Steel Constr* 9(4):323–330
7. Schurgacz P, Knobloch M, Neuenschwander M (2021) Slender column strength of innovative concrete filled steel tube columns with high-performance building materials. In: Knobloch M, Kuhlmann U, Kurz W, Schäfer M (eds) 9th international conference on composite construction in steel and concrete, Stromberg, Germany, 26–30 July
8. Eurocode 8: Design of structures for earthquake resistance – Part 1-1: General rules, seismic actions and rules for buildings; German version EN 1998-1-1:2004 + AC:2009
9. Eurocode 4: Design of composite steel and concrete structures – Part 1-1: General rules and rules for buildings; German version EN 1994-1-1:2004 + AC:2009
10. European Convention for Constructional Steelwork (1986) – Technical Committee 1 – Structural Safety and Loadings Technical Working Group 1.3 – Seismic Design, Recommended Testing Procedure for Assessing the Behaviour of Structural Steel Elements under Cyclic Loads, 1st edn. Report No. 45